Pavel Záskalický, Ján Kaňuch
Faculty of Electrical Engineering and Informatics, Technical University of Košice, Slovakia

ELECTROMAGNETIC TORQUE RIPPLE DIMINUTION OF A FIVE-PHASE ASYNCHRONOUS MOTOR WITH ONE PHASE OPEN CIRCUIT FAULT

REDUKCJA TĘTNIEŃ MOMENTU ELEKTROMAGNETYCZNEGO PIĘCIOFAZOWEGO SILNIKA ASYNCHRONICZNEGO PRZY JEDNOFAZOWEJ UTRACIE MOCY

Abstract: The presented paper deals with the five-phase induction motor (IM) having pentagon connected stator winding, which is working under one phase supply failure. Computation of the motor electromagnetic quantities was made using the space vector theory in the complex plane. Analysis is done assuming, the motor is supplied by a pulse width modulation (PWM) controlled inverter with sufficiently high modulation frequency. Only the first stator voltage harmonics is taken into consideration. On the base of measured IM parameters, trajectories of stator and rotor current space vectors were investigated. On their basis, the motor electromagnetic torque ripple waveform for failure supply mode is derived. Finally a possibility to reduce torque ripple in failure state is shown.

Streszczenie: W artykule opisano pięciofazowy silnik indukcyjny (SI) o pięciokątnym uzwojeniu stojana, pracujący przy jednofazowym zaniku zasilania. Obliczenia wielkości elektromagnetycznych silnika przeprowadzono z wykorzystaniem teorii wektorów przestrzennych na płaszczyźnie zespolonej. Analizę przeprowadzono przy założeniu, że silnik jest zasilany z falownika sterowanego modulacją szerokości impulsów (PWM) o odpowiednio wysokiej częstotliwości modulacji. Uwzględniono tylko pierwszą harmoniczną napięcia stojana. Na podstawie zmierzonych parametrów SI zbadano trajektorie wektorów przestrzeni prądów stojana i wirnika. Na ich podstawie wyznaczono przebieg tętnień momentu elektromagnetycznego silnika dla trybu zasilania awaryjnego. Na zakończenie przedstawiono możliwość redukcji tętnień momentu w stanie awaryjnym.

Keywords: *Five–phase, Induction machine, Torque ripple, Pentagon connection, One phase fault, Four phase operation*
Słowa kluczowe*: Pięciofazowa, maszyna indukcyjna, tętnienie momentu obrotowego, połączenie pięciokątne, uszkodzenie jednofazowe, praca czterofazowa*

1. Introduction

Last time we have been witnessed an increasing interest of multi phase drives for different industrial, automotive and household appliances, because of their supply fault tolerance and high power density. These systems have benefited from development of electronic components for their supply. Complex real-time controls can be achieved thanks to field programmable gate arrays and digital signal processors even in fault-mode configuration. [2], [7]
Multiphase drive are fault tolerant to an opened switch fault or an opened phase fault since a rotating field can be generated. In most cases the effect of a short-circuit fault is destructive and needs either special voltage source inverter or supplementary components. This is the reason why only opened switch or opened phase fault will be considered. Anyhow, impacts of the fault must be carefully studied in term of oversizing induced torque ripples and vibrations that can lead to secondary faults in other parts of the drive system. [12] In the majority cases, supply of the five phase induction motors is provided by a voltage source inverter (VSI). Number of pulse width modulation techniques are available to control VSI output voltage. The space vector PWM technique has become the most popular in these days because of its easy digital implementation and better DC utilization compared to the ramp comparison sinusoidal PWM method. [10]
In previously published statistical studies, the percentage of faults for three-phase variable-speed drives was evaluated to about 60% due to users experiences during the first year of operation. About 70% of these faults were related to

power switches of the VSI, such as short-circuit and open-circuit faults. [3]

2. Inverter modeling

The five phase motors need for their operation a supply from semiconductor converter, which is able to generate five–phase supply voltages. The power circuit topology of the five phase voltage source inverter (VSI) is shown in Fig.1. [4], [8]

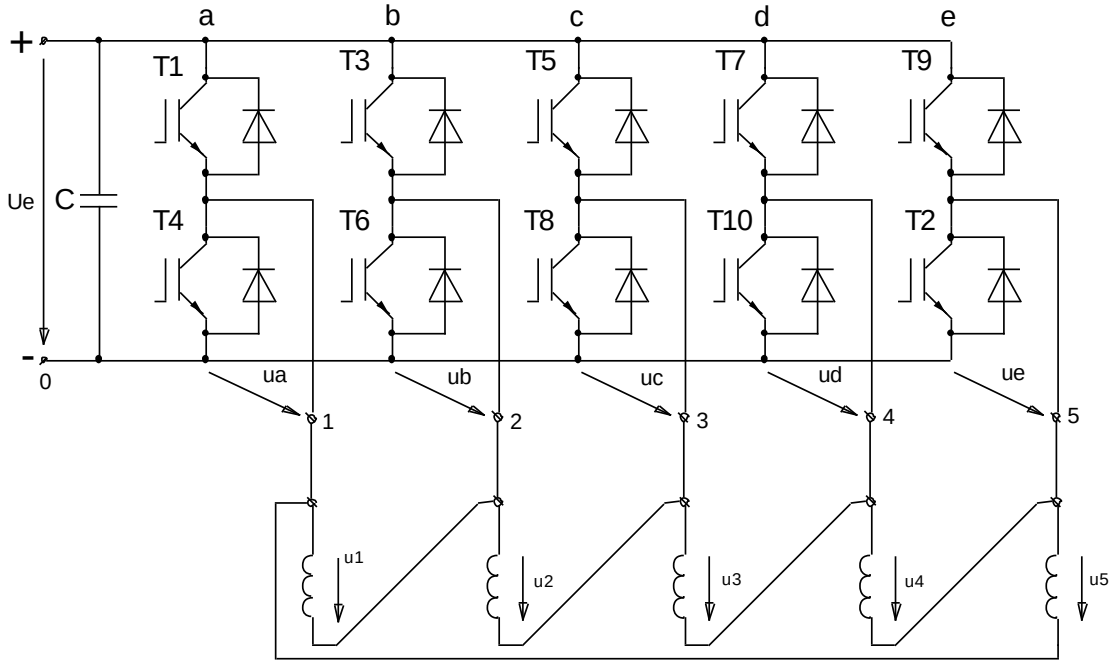

Fig.1. Five–phase bridge connected VSI

VSI consists of parallel connection of five transistor legs. It is supplied by a constant voltage source consisting of an isolated DC-source and a capacitive DC-link. Each leg contains two IGBT transistors with anti-parallel connected freewheeling diodes used to ensure a negative current path through the switches. Inverters output terminals are numbered as 1 − 2 − 3 − 4 − 5. [5], [14], [13]

Steady state mathematical model requires some simplification. In the next step we assume an idealized semiconductor devices which satisfy the following properties:

• power switches can handle unlimited current and they are able to blocks unlimited voltage.

• voltage drop across the switch and the leakage current are zero.

• the switches are turned on and off with no rise and fall times.

• sufficiently big size capacity of the input voltage capacitors divider, to can assume inverter input DC voltage to be constant for any output current.

These assumptions simplify analysis of the power circuit and help to build a steady state mathematical model. Assume that the inverter DC input voltage is constant for any supply current. Next, let's suppose that inverter output voltage is controlled by a PWM with very high modulation frequency (f_m > 10 kHz). On the base of this assumption we can suppose that the inverter output voltages is ideally sinusoidal. Transistors in the first inverters leg are controlled to obtain output leg voltage in the form

$$u_a = u_{dc} + u_{01} = \frac{U_e}{2} + r\frac{U_e}{2}e^{j\omega t} \qquad (1)$$

where, u_{dc} is DC and u_{01} is AC voltage component, r is voltage control coefficient $r \in \langle 0,1 \rangle$ and $\omega = 2\pi f$ is angular frequency.

Leg voltages are measured between the leg nodes and negative rail of the DC supply. The AC voltage components in other legs are shifted gra-

dually by 2π/5. This shift is mathematically expressed by the voltage shifting factor $\mathbf{a} = e^{j\frac{2\pi}{5}}$. Then, we can them express:

$$\begin{aligned} \mathbf{u}_b &= \mathbf{a}\mathbf{u}_a \quad \mathbf{u}_c = \mathbf{a}^2\mathbf{u}_a \\ \mathbf{u}_d &= \mathbf{a}^3\mathbf{u}_a \quad \mathbf{u}_e = \mathbf{a}^4\mathbf{u}_a \end{aligned} \tag{2}$$

Motor phase voltages are given by difference of the voltages between two legs. Since,

$$\mathbf{u}_{dc} = \mathbf{a}\mathbf{u}_{dc} = \mathbf{a}^2\mathbf{u}_{dc} = \mathbf{a}^3\mathbf{u}_{dc} = \mathbf{a}^4\mathbf{u}_{dc}$$

(DC voltage shift), the motor phase voltages can be expressed as:

$$\begin{aligned} \mathbf{u}_1 &= \mathbf{u}_a - \mathbf{u}_b = (\mathbf{a}-1)\mathbf{u}_{ac} \\ \mathbf{u}_2 &= \mathbf{u}_b - \mathbf{u}_c = (\mathbf{a}^2-\mathbf{a})\mathbf{u}_{ac} \\ \mathbf{u}_3 &= \mathbf{u}_c - \mathbf{u}_d = (\mathbf{a}^3-\mathbf{a}^2)\mathbf{u}_{ac} \\ \mathbf{u}_4 &= \mathbf{u}_d - \mathbf{u}_e = (\mathbf{a}^4-\mathbf{a}^3)\mathbf{u}_{ac} \\ \mathbf{u}_5 &= \mathbf{u}_e - \mathbf{u}_a = (1-\mathbf{a}^4)\mathbf{u}_{ac} \end{aligned} \tag{3}$$

Figure 2 depicts the phase voltages formed in the pentagon stator winding connection.

To simplify the calculation of AC motor quantities, it is very advantageous to use space vectors theory. The term ”space” originally stands for the two-dimensional complex plane, to which the multi-phase quantities are transformed. The transformation of space space vector can be directly derived from the sum of voltage phasors. [9]

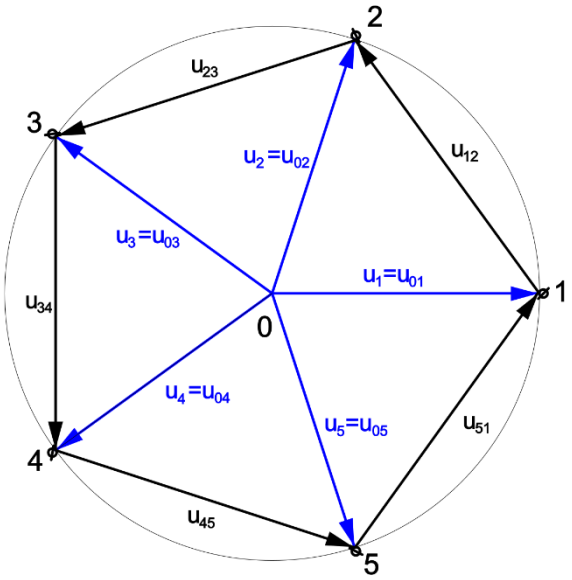

Fig. 2. Pentagon connection voltage phasors

Based on the equation (3), voltage space vector transformation is thus defined as:

$$\underline{\mathbf{u}} = \frac{2}{5}\Big[\mathrm{Re}(\mathbf{u}_1) + \mathbf{a}\,\mathrm{Re}(\mathbf{u}_2) + \mathbf{a}^2\,\mathrm{Re}(\mathbf{u}_3) + \mathbf{a}^3\,\mathrm{Re}(\mathbf{u}_4) + \mathbf{a}^4\,\mathrm{Re}(\mathbf{u}_5)\Big] \tag{4}$$

where, $\mathbf{a} = e^{j\frac{2\pi}{5}}$ is space shifting factor which for pentagon connection is identical with voltage shifting factor. Figure 3 shows the space vector trajectory of the five phase voltage system. This one was calculated on the base of equation (4) for the inverter's DC input value U_e = 550 V. For a symmetric five phase harmonic voltage system, the space vector trajectory forms a circle.

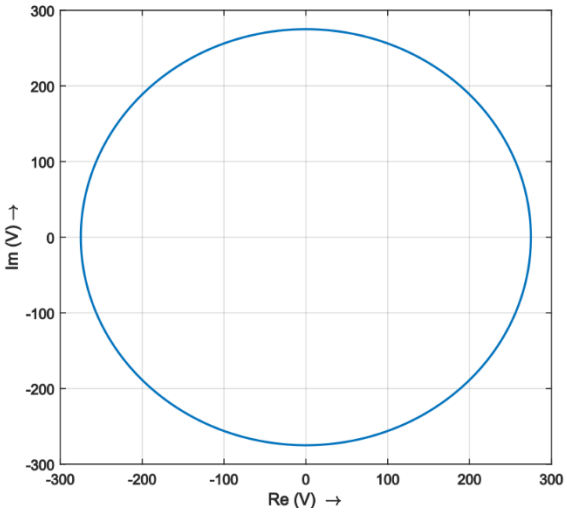

Fig. 3. Voltage space vector trajectory

3. Current space vector

For stator and rotor current space vectors calculation, a classical one phase equivalent circuit of induction machine is advantageously used (Fig. 4). [1], [11]

Motor parameters used for the following calculation are listed in Appendix.

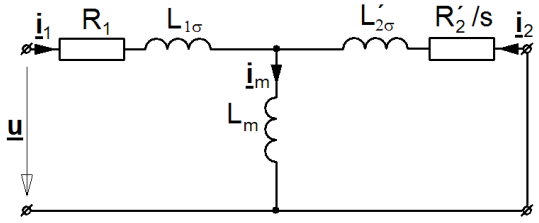

Fig. 4. IM equivalent circuit

Referred to the equivalent circuit above, the following equation for the stator current space vector is valid.

$$\underline{\mathbf{i}}_1 = \frac{\underline{\mathbf{u}}}{R_1 + \left[j\omega L_{1\sigma} + \frac{j\omega L_m \left(R_2'/s + j\omega L_{2\sigma}' \right)}{R_2'/s + j\omega \left(L_m + L_{2\sigma}' \right)} \right]} \quad (5)$$

where, $s = \frac{\omega - p\omega_m}{\omega}$ is the motor slip, $\omega = 2\pi f$ is an angular frequency, ω_m is a motor speed and p is a motor pairs poles.

The rotor current space vector can be determined by using Thevenin theorem. For the rotor current space vector following equation is valid

$$\underline{\mathbf{i}}_2 = -\frac{\frac{U_{th}}{U_e}\underline{\mathbf{u}}}{R_2'/s + R_{th} + j\omega \left(L_{th} + L_{2\sigma}' \right)} \quad (6)$$

where, U_{th} is Thevenin DC input voltage, R_{th} and L_{th} are Thevenin resistance and inductance respectively.

Assume, the motor operates at rating speed, the sleep s = 0.03 and frequency f = 50 Hz. Figure 5 depicts the stator and rotor current space vector trajectories which were calculated on the base of equations (5) and (6).

The electromagnetic torque is calculated on the base of stator and rotor current space vectors

$$M_{em} = \frac{5}{2} pL_m \operatorname{Im}\left(\underline{\mathbf{i}}_1 \underline{\mathbf{i}}_2^* \right) \quad (7)$$

In the Fig. 6 there is shown the time course of electromagnetic torque, calculated on the base of equation (7). In case of a failure-free state the motor electromagnetic torque is constant at all times.

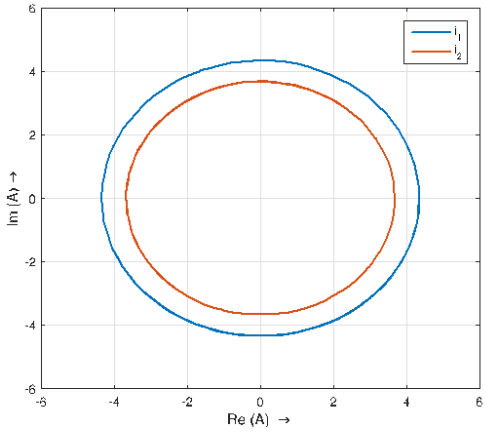

Fig. 5. Stator and rotor current space vector trajectories

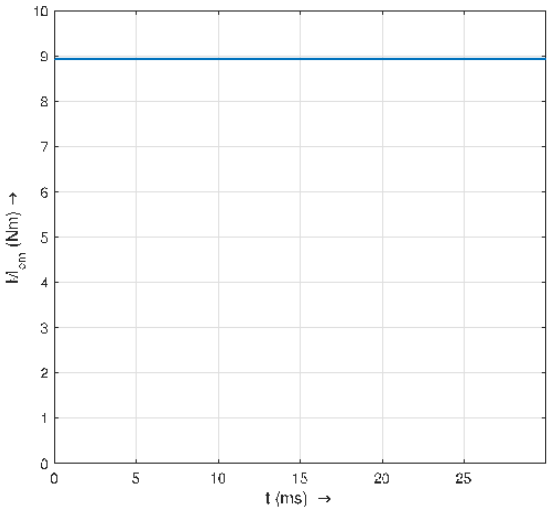

Fig. 6. Electromagnetic torque waveform

4. One-phase failure operation

Let us assume fault on the terminal ”2” - the transistors (T3 − T8) interrupted and ub = 0. Subsequently across the phases ”1” and ”2” there appears the voltage equal to the difference between leg voltages u_a and u_c, as seen in the Figure 7. Assuming symmetry windings in each phase, the voltage is evenly distributed between the phases ”1” and ”2”.

$$\mathbf{u}_1 = \mathbf{u}_2 = \frac{1}{2}\left(\mathbf{u}_c - \mathbf{u}_a \right) = \frac{1}{2}\left(\mathbf{a}^2 - 1 \right)\mathbf{u}_{01} \quad (8)$$

On the base of equation (4) there is possible to calculate voltage space vector trajectory. This one is no longer circular, but elliptical, as depicted in Figure 8.

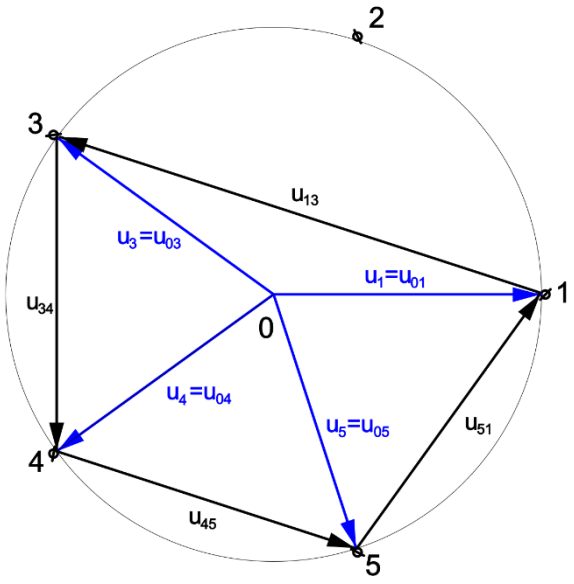

Fig.7. One–phase failure voltage phasors

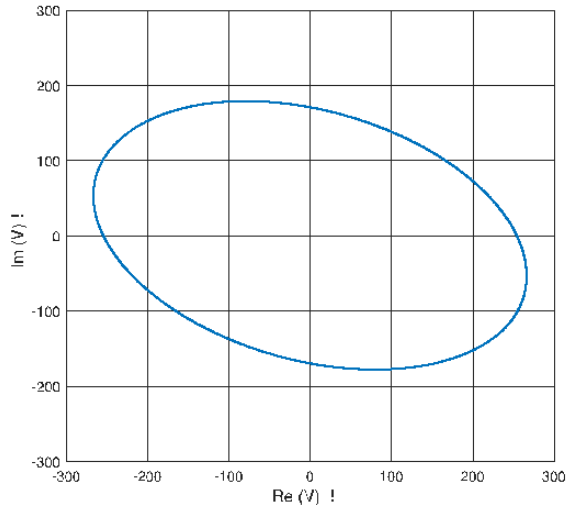

Fig. 8. Voltage space vector trajectory in case of one–phase failure

From equations (5) and (6) the trajectories of stator and rotor current space vector were calculated. They are shown in Figure 9. The calculation was made for supply frequency f = 50 Hz and nominal motor torque. Speed has dropped approximatively by 30 rev/min to the value 2878 rev/min, corresponding to s = 0.0405.

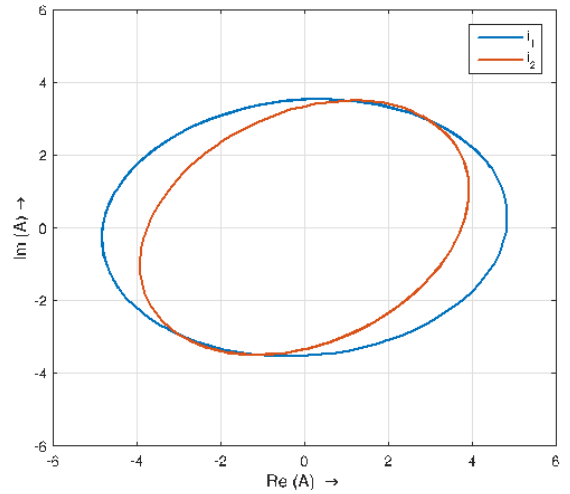

Fig. 9. Current space vectors trajectories in case of one–phase failure

Figure 10 shows calculated electromagnetic torque waveform. This one is strong pulse with second harmonic of the supply voltages frequency. In the calculated waveform, the electromagnetic torque changes within the range ± 30% of nominal value.

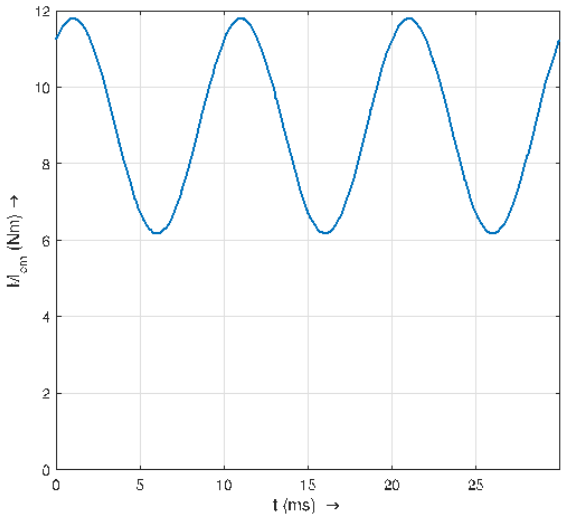

Fig. 10. Electromagnetic torque waveform in case of one–phase failure

5. Electromagnetic torque improvement

As shown above, in case of one phase failure, there is a possibility to smooth the disturbed waveform of the electro-magnetic torque. This can be accomplished by shifting inverter leg voltages ua and uc, as shown in Figure 11. Let us define the fault shifting factor

$$\mathbf{a}_f = e^{j\frac{\pi}{10}} \tag{9}$$

then the shifted leg voltages take the form

$$\mathbf{u}'_{01} = \mathbf{a}_f \mathbf{u}_{01} \quad \mathbf{u}'_{03} = \mathbf{a}_f \mathbf{u}_{03} \tag{10}$$

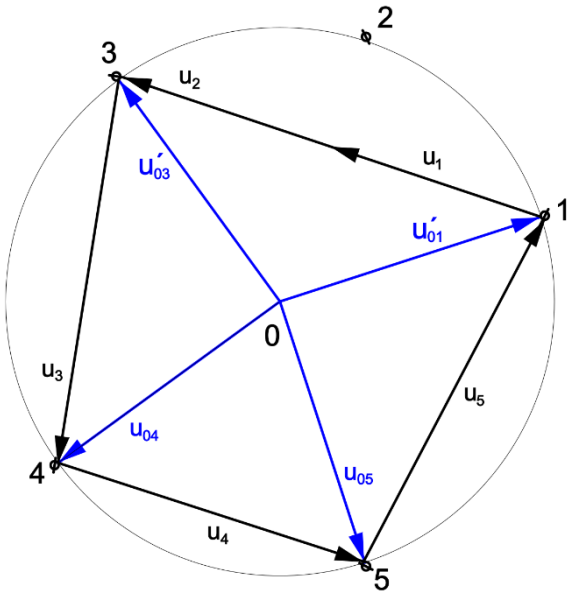

Fig. 11. Shifted voltage phasors

Then, for the motor phase voltages we can write the equations:

$$\mathbf{u}_1 = \mathbf{u}_3 = \frac{1}{2}\left(\mathbf{u}'_{03} - \mathbf{u}'_{01}\right) \quad \mathbf{u}_3 = \mathbf{u}_{04} - \mathbf{u}'_{03} \quad (11)$$
$$\mathbf{u}_4 = \mathbf{u}_{05} - \mathbf{u}_{04} \quad \mathbf{u}_5 = \mathbf{u}'_{01} - \mathbf{u}_{05}$$

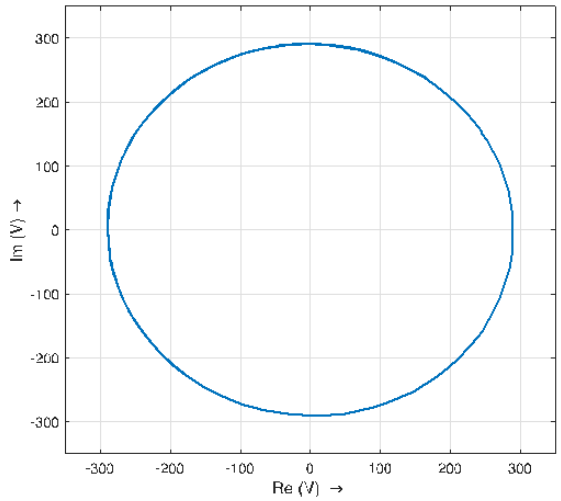

Fig. 12. Shifted voltages space vector trajectory

Figure 12 shows calculated voltage space vector trajectory for three shifted voltages of the five phase IM. This is again circular, but with reduced voltage amplitude. It can be seen in Fig. 13 that the currents trajectories are circular too, for nominal load but is stator winding slightly overloaded.

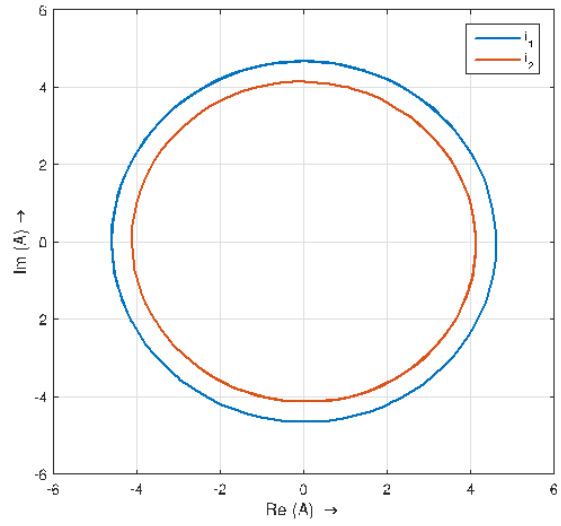

Fig. 13. Shifted currents space vector trajectories

Figure 14 depicts, that electromagnetic torque is practically constant. The ripple (± 0.12 Nm) presents only little more than 1 % of nominal value.

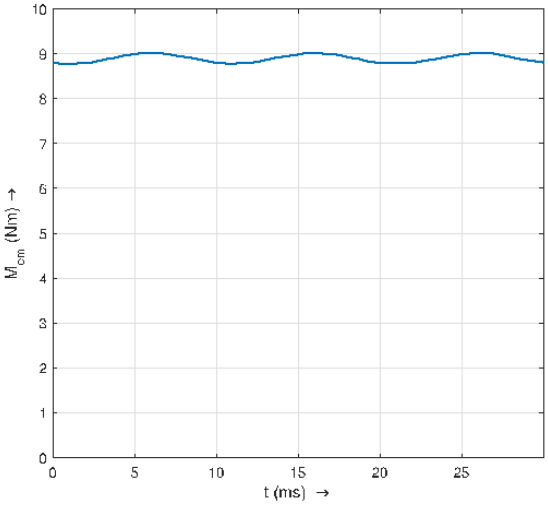

Fig. 14.Shifted voltages electromagnetic torque vaweform

6. Conclusion

The paper deals with the five-phase induction motor (IM) with pentagon connected stator winding, which is working under one phase supply failure. The space vector theory was used for computation of motor electromagnetic quantities.

A new algorithm for PWM–VSI control of five-phase IM machine in a case of one supply phase failure was proposed. It needs only to measure output inverter currents that are already available for a closed-loop control of the electric drive, avoiding thus any use of additional sensors, complex hardware or calculations. The most important goal is to achieve a renewal for the continuity of electric drive operation.

It is shown, that in case of the fault state there is possible switch motor to a four-phase operation state and minimize electromagnetic torque ripple. In any case, the motor loses its original performance power, but it is capable to work in smooth operation.

Appendix

Five phase induction motor parameters:

P_n = 1,75 kW; Un = 5 × 230 V/50 Hz; n_n = 2910 rev/min.; p = 1; R_1 = 3,778 Ω; R'_2 = 2,485 Ω; Lm = 0,436 H; $L_1\sigma$ = 6,83 mH; $L_2\sigma$ = 6,83 mH;

Acknowledgment

The author would like to thank Slovak Research and Development Agency for financial support. Paper was made under the contract No: APVV-16-0270 and APVV-19-210

References

[1]. J. Chatelain, “Machines electriques”, Vol. X, Edition Georgi, 1983.
[2]. M. Trabelsi, N. K. Nguyen, E. N. Semail, “Real-Time Switches Fault Diagnostics Based on Typical Operating Characteristics of Five-Phase Permanent-Magnetic Synchronous Machines,” IEEE Transactions on Industrial Electronics, Vol. 63, No. 8, pp. 4683–4694, 2016.
[3]. R. A. Hanna, S. Prabhu, “Medium-voltage adjustable-speed drives users and manufactures,” IEEE Trans. Ind. Appl., Vol. 33, No. 6, pp. 1407– 1415, 1997.
[4]. M. Frivaldsky, B. Dobrucký, M. Praženica, J. Koscelníik, “Multi-tank resonant topologies as key design factors for reliability improvement of power converter for power energy applications”, Electrical Engineering - Archiv fur Elektrotechnik, SPRINGER, Vol. 97, No. 4, pp. 287–302, ¨ 2015.
[5]. P. Zaskalicky, “Mathematical Model of a Five-phase Voltage-source PWM Controlled Inverter”, Electrical Engineering - Archiv fur Elek- ¨ trotechnik, SPRINGER, No. 99, pp. 1179-1184, 2017.
[6]. P. Zaskalicky, “Behavior of a Five-Phase Pentacle Connected IM Operated under One-Phase Fault”, ACEMP-OPTIM Conference, 27–29. august 2019, Istanbul, Turkey.
[7]. R. Ganiev, “Reversible frequency converters in the composition of multimotor electric drives”, IOP Conference Series: Materials Science and Engineering, Volume 643, Issue 1, 13 November 2019, Institute of Energy and Transport System, Peter the Great Saint Petersburg Polytechnic University Saint Petersburg; Russian Federation; 23- 24 May 2019.
[8]. B. Dobrucky, S. Kascak, M. Prazenica, “A novel enhanced connection of AC/AC power train for HEV-Modelling and simulation results”, Advances in Electrical and Electronic Engineering 16(3), pp. 253–260, 2018.
[9]. H.M. Ryu, S.K. Sul, “Multiple d-q spaces concept for multi-phase AC motor drive”, ICPE–04, pp. 670–674, 2004.
[10]. E. Levi, “Multiphase electric machines for variable–speed applications”, IEEE Trans. on Ind. Electronics, Vol. 55, No. 5, pp. 1893-1909, 2008.
[11]. D. Balara, J. Timko, J. Zilkov ˇ a, M. Le ´ so, “Neural networks application ˇ for mechanical parameters identification of asynchronous motor”, Neural Network World, Vol. 27, No. 3, pp. 259-315, 2017.
[12]. J.O. Estima, A.J. Marques Cardoso, “A new algorithm for real-time multiple open-circuit fault diagnostic in voltage-fed PWM motor drives by the reference currents errors”, IEEE Trans. on Ind. Electronics, Vol. 28, No. 5, pp. 3496-3505, 2013.
[13]. V. Šlapak, K. Kyslan, F. Durovsky, “Position Controller for PMSM Based on Finite Control Set Model Predictive Control”, Elektronika Ir Elektrotechnika, vol. 22, No. 6, pp. 81–85, 2017.